Dispersion curves in the diffusional instability of reaction fronts

Article (Published Version)

Dispersion curves in the diffusional instability of autocatalytic reaction fronts

J. H. Merkin[1] and I. Z. Kiss[2]
[1]*Department of Applied Mathematics, University of Leeds, Leeds, LS2 9JT, United Kingdom*
[2]*Department of Zoology, University of Oxford, Oxford OX1 3PS, United Kingdom*
(Received 21 March 2005; revised manuscript received 19 May 2005; published 24 August 2005)

A (linear) stability analysis of planar reaction fronts to transverse perturbations is considered for systems based on cubic autocatalysis and a model for the chlorite-tetrathionate reaction. Dispersion curves (plots of the growth rate σ against a transverse wave-number k) are obtained. In both cases it is seen that there is a nonzero value D_0 of D (the ratio of the diffusion coefficients of autocatalyst and substrate) at which σ_{max}, the maximum value of σ for a given value of D, achieves its largest value, with σ_{max} being less for other values of D and becoming small as D decreases to zero. The existence of the optimum value D_0 for initiating a diffusional instability is confirmed, in the cubic autocatalysis case, by an asymptotic analysis for small wave numbers.

DOI: 10.1103/PhysRevE.72.026219 PACS number(s): 82.40.Bj, 82.40.Ck, 89.75.Fb

I. INTRODUCTION

It is already well-established, both experimentally [1–3] and theoretically [4,5], that planar reaction fronts in autocatalytic systems can become transversely unstable if the diffusion coefficients of substrate and autocatalyst differ by a sufficient amount. Much of this previous work has been concerned with the iodate-arsenous acid (IAA) system, for which cubic autocatalysis is a good approximation in the arsenous acid excess case [6]. It is this latter reaction we consider in detail, namely,

$$A + 2B \rightarrow 3B \quad \text{rate } k_0 ab^2, \tag{1}$$

where a and b are the concentrations of A and B, respectively, and k_0 is a constant. For the IAA system, A and B represent, respectively, IO_3^- and I^-. The dimensionless reaction-diffusion equations corresponding to reaction (1) are (see, [7,8], for example)

$$\frac{\partial a}{\partial t} = \nabla^2 a - ab^2, \quad \frac{\partial b}{\partial t} = D\nabla^2 b + ab^2, \tag{2}$$

where $D = D_B/D_A$ is the ratio of the diffusion coefficients of reactant species B and A. Ahead of the reaction front there is only A present and, in the front, A is converted fully to B.

The basic idea, as described clearly in [4], is that the diffusion of the autocatalyst B has a stabilizing effect on planar waves, whereas the diffusion of the substrate A has a destabilizing effect. Thus if this latter effect is sufficiently strong relative to the first, i.e., if the ratio D is sufficiently different from unity, then the wave will become transversely unstable. This leads to a critical value D_c of D at which the stability of a planar wave changes, with, in the present description (2), the wave being unstable for $D < D_c$. For cubic autocatalysis it has been shown [5] that $D_c \simeq 0.435$.

From this argument, it might be expected that the instability should strengthen as the difference $|D_c - D|$ increases, as exemplified, for example, by increasing (positive) growth rates σ derived in a linear stability analysis. We find that this is not the case when we compute the dispersion curves, i.e., plots of σ against a transverse wave-number k for a given value of D. We see that the maximum value of the growth rate σ_{max} starts by increasing as D is reduced from D_c. However, a value of D_0 of D is reached at which point σ_{max} achieves its greatest value, with $D_0 \simeq 0.15$ for cubic autocatalysis. For values of $D < D_0$, the value of σ_{max} decreases as D is further reduced from D_c and becomes very small for small values of D.

Our analysis is based on the linear stability of planar reaction fronts in system (1) governed by Eqs. (2) and we now derive the equations for this analysis.

II. STABILITY ANALYSIS

We have in mind the experiments performed in Hele-Shaw cells and the consequent theory, see [10–13], for example. This allows us to restrict attention to two space variables, x in the direction of propagation and y transverse to the reaction front. The planar traveling waves, the base state for our stability analysis, are determined from Eq. (2) by first introducing the traveling coordinate $\zeta = x - ct$, where $c(>0)$ is the (constant) wave speed and then looking for a solution in the form

$$a(x,y,t) = a_0(\zeta), \quad b(x,y,t) = b_0(\zeta). \tag{3}$$

The resulting traveling wave equations are

$$a_0'' + ca_0' - a_0 b_0^2 = 0, \quad Db_0'' + cb_0' + a_0 b_0^2 = 0, \tag{4}$$

(where primes denote differentiation with respect to ζ), being subject to the boundary conditions

$$a_0 \rightarrow 1, \quad b_0 \rightarrow 0 \text{ as } \zeta \rightarrow \infty, \quad a_0 \rightarrow 0, \quad b_0 \rightarrow 1 \text{ as } \zeta \rightarrow -\infty. \tag{5}$$

Equations (4) and (5) have already been discussed in some detail [9,8]. For completeness we show a graph of the wave speed c plotted against D in Fig. 1. We note that $c \sim 1.219D + \cdots$ as $D \rightarrow 0$ [9] (shown by the broken line in Fig. 1).

To consider the diffusional stability of the reaction fronts given by Eqs. (4) and (5), we put

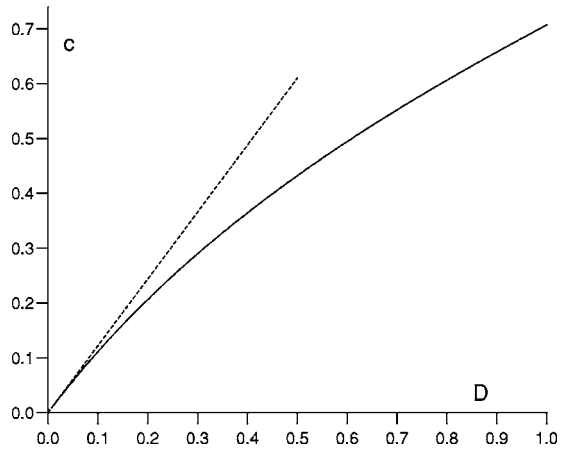

FIG. 1. The speed c of the reaction fronts, as given by Eqs. (4) and (5), plotted against D. The asymptotic solution given in [9] is shown by the broken line.

$$a(\zeta,y,t) = a_0(\zeta) + A(\zeta,y,t), \quad b(\zeta,y,t) = b_0(\zeta) + B(\zeta,y,t), \tag{6}$$

where we assume that A, B are small perturbations. We substitute Eq. (6) into Eqs. (2) and look for a solution in the form

$$A(\zeta,y,t) = \mathrm{e}^{\sigma t + iky}\bar{A}(\zeta), \quad B(\zeta,y,t) = \mathrm{e}^{\sigma t + iky}\bar{B}(\zeta). \tag{7}$$

This leads to an eigenvalue problem for $[\bar{A}(\zeta), \bar{B}(\zeta)]$ in terms of the growth rate σ and the wave-number k as

$$\bar{A}'' + c\bar{A}' - (b_0^2 + k^2 + \sigma)\bar{A} - 2a_0b_0\bar{B} = 0 \tag{8}$$

$$D\bar{B}'' + c\bar{B}' - (Dk^2 - 2a_0b_0 + \sigma)\bar{B} + b_0^2\bar{A} = 0 \tag{9}$$

subject to the boundary conditions that

$$\bar{A} \to 0, \quad \bar{B} \to 0, \quad \text{as } \zeta \to \pm\infty. \tag{10}$$

We note in passing that, when $D=1$, $a_0+b_0 \equiv 1$, $\bar{A}+\bar{B} \equiv 0$ and, as a consequence, $\sigma=-k^2$.

For general values of D, Eqs. (8)–(10) had to be solved numerically, which was done using the technique described in [13,14]. The traveling wave Eqs. (4) and (5) were solved using a shooting technique incorporating the asymptotic forms of the solution for $|\zeta|$ large. The concentration profiles were then specified at N points with equally spacing $\Delta\zeta$. Equations (8) and (9) were then discretized at these N points using central-difference approximations for the derivatives. This converts the system to an $N \times N$ matrix eigenvalue problem, which was solved using the LAPACK solver DGEEVX. For our results we generally used $N=500$ and $\Delta\zeta=0.1$, although some cases were calculated with a larger N (and smaller $\Delta\zeta$) to check accuracy. From these calculations the largest eigenvalue σ is determined for a given value of the wave-number k. Repeating these calculations for different values of the wave number enables the dispersion curves to be plotted.

In Fig. 2 we plot dispersion curves for a range of values of D. In Fig. 2(a) (for $D=1.0$ to $D=0.1$) we see that the reaction front becomes transversely unstable, i.e., $\sigma>0$ for a range of k, at a value between $D=0.5$ and $D=0.4$, consistent with [5]. Also, the (positive) maximum value of σ increases as D is decreased to $D=0.1$. In Fig. 2(b) we give dispersion curves for $D=0.1$ to $D=0.025$. In this case we see that σ_{max} *decreases* as D is decreased from $D=0.1$, although the range of unstable wave numbers is increasing. The maximum value of σ has become relatively small by $D=0.025$ and suggests that possibly $\sigma_{max} \to 0$ as $D \to 0$ (a point that is confirmed below). To emphasise this point we give the values of σ_{max} obtained from these dispersion curves against D in Fig. 3(a). This figure indicates that σ_{max} achieves its greatest value at $D=D_0 \simeq 0.15$. (Note that we have plotted $10^2 \times \sigma_{max}$ in this figure.) In Fig. 3(b) we give the corresponding values of the wave-number k_{max} where $\sigma=\sigma_{max}$. The figure shows that k_{max} decreases as D increases (as seen in Fig. 2), from $k_{max} \simeq 0.249$ at $D=0.025$ to $k_{max} \simeq 0.073$ at $D=0.4$.

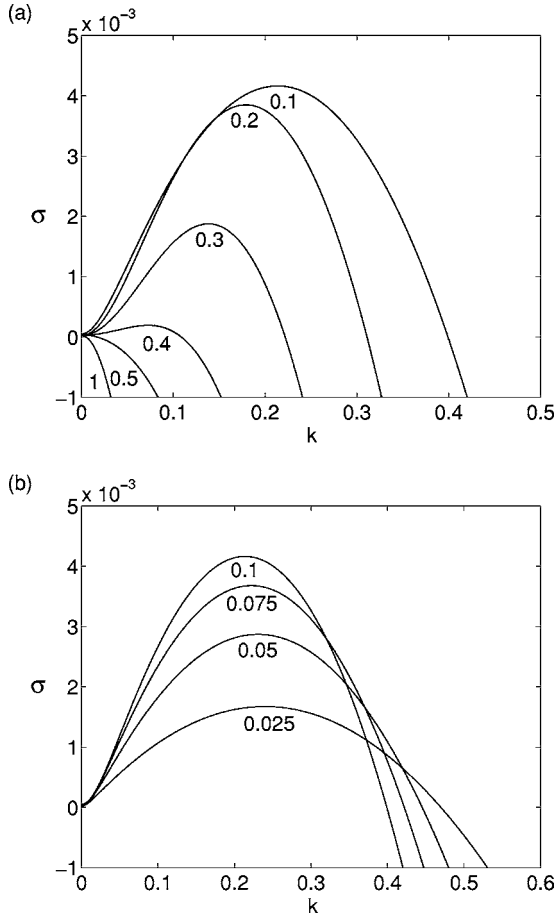

FIG. 2. Dispersion curves for cubic autocatalysis (1), plots of σ against k, obtained from Eqs. (8)–(10), (a) for $D=1.0$ to $D=0.1$, (b) for $D=0.1$ to $D=0.025$.

We can gain further insight into the nature of these dispersion curves by considering the solution to Eqs. (8) and (9) for k small, which is what we now do.

A. Solution for small wave numbers

We look for a solution to Eqs. (8)–(10) (for $D \neq 1$) valid for k small by expanding

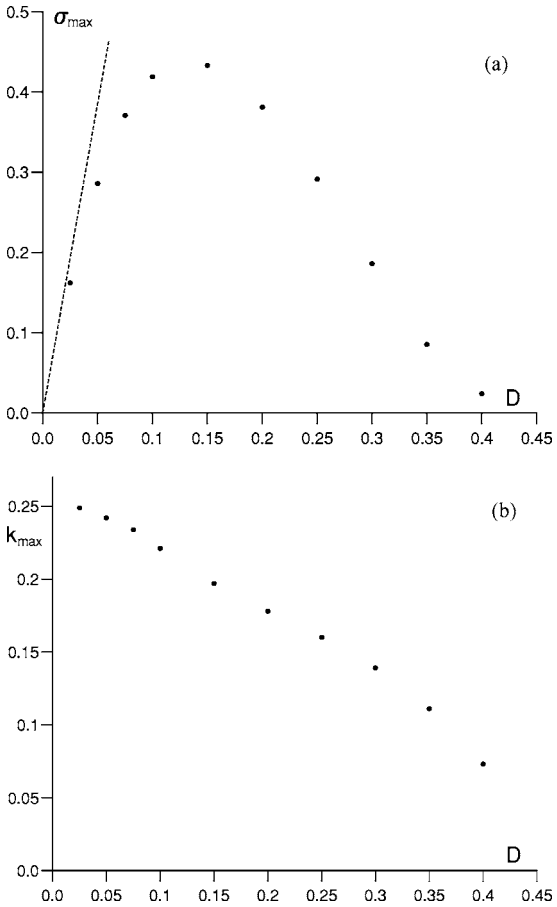

FIG. 3. (a) Values of $\sigma_{max}\times 10^2$ obtained from the dispersion curves shown in Fig. 2 plotted against D to show that σ_{max} achieves its largest value at $D\simeq 0.15$. (b) The values of the wave-number k_{max} where $\sigma=\sigma_{max}$.

$$\bar{A}(\zeta;k) = A_0(\zeta) + k^2 A_1(\zeta) + \cdots,$$

$$\bar{B}(\zeta;k) = B_0(\zeta) + k^2 B_1(\zeta) + \cdots, \quad \sigma(k) = \sigma_0 k^2 + \sigma_1 k^4 \cdots. \tag{11}$$

It is easily seen that the solution to the leading order problem is

$$A_0 = a_0'(\zeta), \quad B_0 = b_0'(\zeta), \tag{12}$$

which simply reflects the fact that Eqs. (4) are translationally invariant. Any arbitrary multiple of Eq. (12) is also a solution to the leading order problem and, without any loss in generality, we can take this to be unity.

At $O(k^2)$ we obtain, using Eq. (12),

$$A_1'' + cA_1' - b_0^2 A_1 - 2a_0 b_0 B_1 = (\sigma_0 + 1)a'_0,$$

$$DB_1'' + cB_1' + 2a_0 b_0 B_1 + b_0^2 A_1 = (\sigma_0 + D)b'_0. \tag{13}$$

Before examining the solution to Eqs. (13) in detail, we first note that, on adding the equations, integrating once and applying the boundary conditions that $A_1\to 0, B_1\to 0$ as $\zeta\to\infty$,

$$A_1' + cA_1 + DB'_1 + cB_1 = (\sigma_0 + 1)(a_0 - 1) + (\sigma_0 + D)b_0. \tag{14}$$

Equation (14) shows that we cannot also apply the boundary conditions that $A_1\to 0, B_1\to 0$ as $\zeta\to-\infty$. The most we can do is to satisfy

$$A_1 \to 0, \quad B_1 \to \frac{(D-1)}{c} \text{ as } \zeta \to -\infty. \tag{15}$$

Conditions (15) reflect the singular nature of the solution to Eqs. (8) and (9) as $k\to 0$. To complete the solution an outer region is required in which

$$Y = k^2\zeta, \quad a_0 \equiv 0, \quad b_0 \equiv 1, \quad \bar{A} \equiv 0, \quad \bar{B} = k^2\tilde{B}(Y;k),$$

$$\sigma = k^2\tilde{\sigma}. \tag{16}$$

The resulting equation for $\tilde{B}$ is

$$k^2 D\tilde{B}'' + c\tilde{B}' - (\tilde{\sigma} + D)\tilde{B} = 0. \tag{17}$$

In Eq. (17) primes denote differentiation with respect to Y. A solution is sought by expanding in powers of k^2, the leading order solution $\tilde{B}_0$ is, on matching with Eq. (15) and using Eq. (11)

$$\tilde{B}_0 = \frac{(D-1)}{c}\exp\left(\frac{(\sigma_0 + D)}{c}Y\right). \tag{18}$$

We note that $\tilde{B}_0\to 0$ as $Y\to-\infty$ and is consistent with the behavior, as $\zeta\to-\infty$, of the solution to the equations that arise at $O(k^4)$ in expansion (11).

We now return to Eqs. (13). We note that $A_1=a_0'$, $B_1=b_0'$ is a solution to the homogeneous problem satisfying homogeneous boundary conditions. Thus a compatibility condition is required for the nonhomogeneous problem to have a solution which satisfies all the boundary conditions. It is this condition that determines the constant σ_0. To derive this condition we need to consider the adjoint problem [16] (Theorem 2.2, page 307). To do so we start by writing Eqs. (13) in the form

$$\frac{d}{d\zeta}(e^{c\zeta}A_1') - (b_0^2 A_1 + 2a_0 b_0 B_1)e^{c\zeta} = (\sigma_0 + 1)e^{c\zeta}a_0',$$

$$\frac{d}{d\zeta}(De^{c\zeta/D}B_1') + (b_0^2 A_1 + 2a_0 b_0 B_1)e^{c\zeta/D} = (\sigma_0 + D)e^{c\zeta/D}b_0'. \tag{19}$$

We then write $w_1=e^{c\zeta}A_1'$, $w_2=De^{c\zeta/D}B_1'$ and express Eqs. (19) as the system of first-order equations

$$\mathbf{u}' = M\mathbf{u} + \mathbf{R}, \tag{20}$$

where

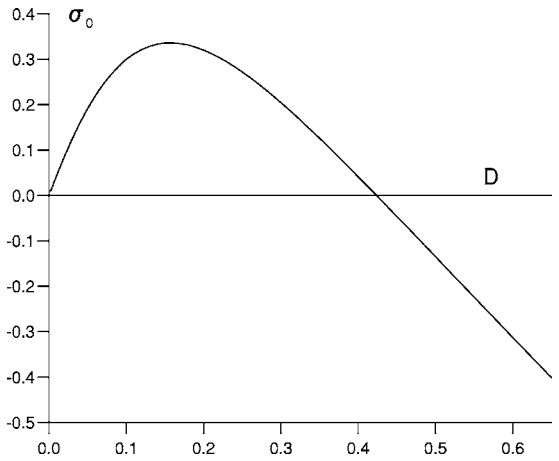

FIG. 4. The analysis for small k, values of σ_0 obtained from the compatibility condition (24) plotted against $D(\sigma \sim \sigma_0 k^2)$.

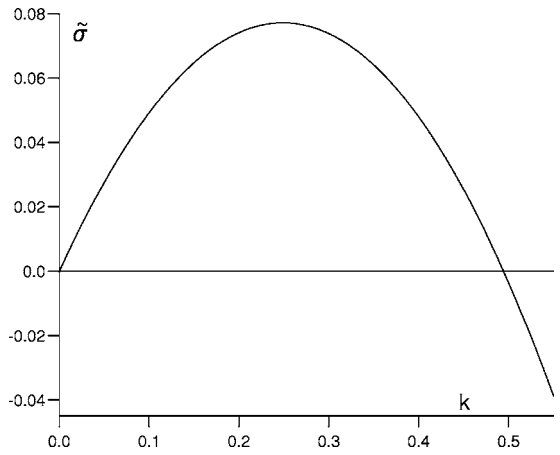

FIG. 5. Dispersion curve $\tilde{\sigma}$ against k obtained from Eq. (27) for small D analysis.

$$\mathbf{u} = \begin{pmatrix} A_1 \\ B_1 \\ w_1 \\ w_2 \end{pmatrix}, \quad \mathbf{R} = \begin{pmatrix} 0 \\ 0 \\ (\sigma_0 + 1)e^{c\zeta} a_0' \\ (\sigma_0 + D)e^{c\zeta/D} b_0' \end{pmatrix},$$

$$M = \begin{pmatrix} 0 & 0 & e^{-c\zeta} & 0 \\ 0 & 0 & 0 & D^{-1}e^{-c\zeta/D} \\ b_0^2 e^{c\zeta} & 2a_0 b_0 e^{c\zeta} & 0 & 0 \\ -b_0^2 e^{c\zeta/D} & -2a_0 b_0 e^{c\zeta/D} & 0 & 0 \end{pmatrix}.$$

The adjoint problem is then [16]

$$\mathbf{v}' = -M^T \mathbf{v}. \tag{21}$$

If we put $\mathbf{v} = (z_1, z_2, U, V)^T$ in Eq. (21), we obtain the required adjoint problem, on eliminating z_1, z_2,

$$\frac{d}{d\zeta}(e^{c\zeta} U') - b_0^2 (e^{c\zeta} U - e^{c\zeta/D} V) = 0,$$

$$\frac{d}{d\zeta}(D e^{c\zeta/D} V') - 2a_0 b_0 (e^{c\zeta} U - e^{c\zeta/D} V) = 0, \tag{22}$$

subject to

$$U, V \to 0 \text{ as } \zeta \to \pm\infty. \tag{23}$$

The compatibility condition $\int_{-\infty}^{\infty} \mathbf{v}^T \cdot \mathbf{R} d\zeta$ then gives

$$(\sigma_0 + 1) \int_{-\infty}^{\infty} e^{c\zeta} a_0' U d\zeta + (\sigma_0 + D) \int_{-\infty}^{\infty} e^{c\zeta/D} b_0' V d\zeta = 0. \tag{24}$$

It is condition (24) that determines σ_0.

The adjoint problem (22) and (23) has to be solved numerically. This was found to be a relatively straightforward process applying the same shooting method that was used for the traveling wave Eqs. (4) and (5). Having calculated U and V, these were then used to calculate the integrals in Eq. (24) to determine σ_0. A graph of σ_0 against D is shown in Fig. 4. This graph shows that $\sigma_0 = 0$ at $D = 0.4236$. (This value was obtained by refining the numerical procedure to take very small increments in D around this value.) The graph also shows that $\sigma_0 \to 0$ as $D \to 0$, and that σ_0 reaches its maximum value of $\sigma_0 = 0.34$ at $D = 0.16$. These results are consistent with [5] and the dispersion curves shown in Fig. 2. These dispersion curves have a "parabolic" appearance in the unstable region. This suggests that we could use σ_0 as an alternative measure of the strength of the diffusional instability (note that $\sigma \sim \sigma_0 k^2$ for k small and so σ_0 gives the "slope" of the dispersion curve at the origin). Using this criterion, our results indicate that $D_0 = 0.16$ is the optimum value of D for the growth of a diffusional instability.

B. Solution for D small

The results shown in Fig. 2 (and in Fig. 6 below) suggest that σ becomes small as D decreases toward zero. We can obtain a solution valid for $D \ll 1$ following directly on from the approach used in [9] for the traveling wave equations. The transformation $a_0(\zeta) = D\tilde{a}_0(\zeta)$, $c = \tilde{c}D$ was applied in [9] to obtain the leading order equations for the traveling wave solution in the inner region

$$\tilde{a}_0'' - \tilde{a}_0 b_0^2 = 0, \quad b_0'' + \tilde{c} b_0 + \tilde{a}_0 b_0^2 = 0, \tag{25}$$

subject to the boundary conditions that

$$\tilde{a}_0 \to 0, \quad b_0 \to 1 \text{ as } \zeta \to -\infty, \quad \tilde{a}_0 \sim \tilde{c}\zeta + \cdots,$$
$$b_0 \to 0 \text{ as } \zeta \to \infty. \tag{26}$$

An outer region, in which $\bar{\zeta} = D\zeta$, $b_0 = D^2 \overline{b_0}$, is then required to complete the solution. However, it is the solution in the inner region that determines $\tilde{c}$ ([9] found $\tilde{c} = 1.219$) and it is this region that concerns us for the stability analysis.

In the inner region we also put $\sigma = D\tilde{\sigma}$, $\bar{A} = D\tilde{A}$, which results in the leading order equations for the stability analysis for $D \ll 1$ from Eqs. (8) and (9)

$$\tilde{A}'' - (b_0^2 + k^2)\tilde{A} - 2\tilde{a}_0 b_0 \bar{B} = 0,$$

$$\bar{B}'' + \tilde{c}\bar{B}' + b_0^2 \tilde{A} + (2\tilde{a}_0 b_0 - k^2 - \tilde{\sigma})\bar{B} = 0, \qquad (27)$$

still subject to conditions (10). Equations (27) were solved numerically using the traveling wave solution given by Eqs. (25) and (26), to determine $\tilde{\sigma}$ in terms of k, with a graph of $\tilde{\sigma}$ being given in Fig. 5. This graph has a similar shape to those given in Fig. 2, although now $\sigma = D\tilde{\sigma}$. Values of $\tilde{\sigma}$ reach a maximum value of $\tilde{\sigma}_{max} = 0.0772$, so that $\sigma_{max} \sim 0.0772\ D + \cdots$ as $D \to 0$. This asymptotic form is shown in Fig. 3(a) by the broken line and shows reasonable agreement with the results for the smaller values of D. The graph also shows that $\tilde{\sigma} = 0$ at $k = 0.494$, which provides an upper bound for the possibility of unstable wave numbers.

III. DISCUSSION

We have established, both through the numerical calculation of dispersion curves and by an analysis for small wave numbers, that there is an optimum value D_0 of D (the ratio of the diffusion coefficients of autocatalyst to substrate) for the generation of a diffusional instability. By this we mean that, with $D = D_0$, the growth rates σ arising in a linear stability analysis achieve their largest values, with only smaller maximum growth rates being reached for other values of $D(< D_c)$. In fact, we have shown that the growth rates are of $O(D)$ for D small, with $\sigma_{max} \sim 0.0772\ D$ as $D \to 0$. Alternatively, there is a nonzero value of the diffusion coefficient D_B of the autocatalyst which makes the system most unstable. This result appears contrary to the argument previously employed in [4] to show the possibility of diffusional instabilities. This argument is essentially the same as that given for a Turing instability and, in this scenario, the system does become increasingly unstable (in the sense we have used) as it moves away from criticality.

A diffusional instability arises when the flux of the reactant is sufficiently greater than that of the autocatalyst. When the diffusion coefficient of the autocatalyst is decreased (smaller values of D) the overlap of reactant and autocatalyst decreases, resulting in lower reaction rates and slower front speeds (see Fig. 1). Thus there are two counteracting effects. Whereas the decrease in the flux of the autocatalyst favors the instability, the decrease in the reaction rates for the autocatalysis leads to a weaker feedback, tending to slow the growth of the instability. This latter effect becomes more pronounced at the smaller values of D and accounts for the decrease in σ at these values (as in Figs. 2, 3, and 6). Applying electric fields to the system has been shown previously to lead to similar effects, producing changes in the concentration fluxes and consequent changes in the stability characteristics, see, for example, [17–19].

Our discussion has concentrated on cubic autocatalysis (1) and an obvious question is whether the optimum value $D_0 > 0$ of D for initiating a diffusional instability is particular to this system or a more general feature. To go a little way to address this point we also computed dispersion curves for the chlorite-tetrathionate (CT) system, which we modeled by a two-variable reaction mechanism for the species $[S_4O_6^{2-}] \equiv a$ and $[H^+] \equiv b$ [15]. In dimensionless variables this results in the reaction-diffusion equations [13] [following (2)]

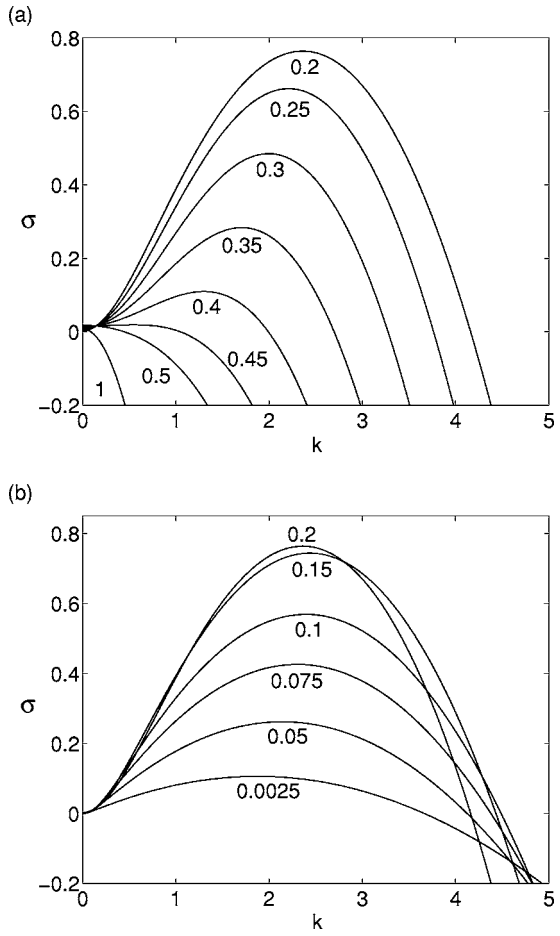

FIG. 6. Dispersion curves for the chlorite-tetrathionate system (28), plots of σ against k, (a) for $D = 1.0$ to $D = 0.2$, (b) for $D = 0.2$ to $D = 0.0025$.

$$\frac{\partial a}{\partial t} = \nabla^2 a - ab^2(\kappa + 7a), \quad \frac{\partial b}{\partial t} = D\nabla^2 b + 6ab^2(\kappa + 7a), \qquad (28)$$

where we took $\kappa = 1$ in the computations (following [13]). The planar traveling wave solutions to Eq. (28) have already been fully discussed in [13] and we used these as our base state in a linear stability analysis for transverse diffusional instabilities. The resulting dispersion curves are shown in Fig. 6. In Fig. 6(a) we give the curves for $D = 1.0$ to $D = 0.2$. This figure shows that an instability develops (a range of k over which $\sigma > 0$) around $D = 0.45$ and the growth rates σ increase as D is reduced to $D = 0.2$. In Fig. 6(b) we give the dispersion curves for $D = 0.2$ to $D = 0.0025$. Here we observe the same general feature as for cubic autocatalysis (compare with Fig. 2), with the growth rates decreasing as

D is decreased. Again the growth rates σ become small as D gets very small. For the CT system there is also the existence of a (nonzero) optimum value D_0 (here $D_0 \simeq 0.2$) at which σ_{max} achieves its largest value, hence making the system most unstable at this value of D.

Although our results are for two relatively simple chemical systems (IAA and CT), they do suggest that the existence of a nonzero value of the ratio of diffusion coefficients at which the system is most unstable to diffusional instabilities could well be a general feature of this type of system.

ACKNOWLEDGMENTS

We wish to thank Brian Sleeman for pointing out how to calculate the adjoint problems (20) and (21). I.Z.K. wishes to thank ORS and the University of Leeds for financial support.

[1] D. Horváth and K. Showalter, J. Chem. Phys. **102**, 2471 (1995).
[2] D. Horváth and A. Tóth, J. Chem. Phys. **108**, 1447 (1998).
[3] M. Fuentes, M. N. Kuperman, and P. De Kepper, J. Phys. Chem. A **105**, 6769 (2001).
[4] D. Horváth, V. Petrov, S. K. Scott, and K. Showalter, J. Chem. Phys. **98**, 6332 (1993).
[5] A. Malevanets, A. Careta, and R. Kapral, Phys. Rev. E **52**, 4724 (1995).
[6] J. H. Merkin and H. Ševčíková, Phys. Chem. Chem. Phys. **1**, 91 (1999).
[7] J. Billingham and D. J. Needham, Dyn. Stab. Syst. **6**, 33 (1991).
[8] D. J. Needham and J. H. Merkin, Nonlinearity **5**, 413 (1992).
[9] J. Billingham and D. J. Needham, Philos. Trans. R. Soc. London, Ser. A **334**, 1 (1991).
[10] M. Böckmann and S. C. Müller, Phys. Rev. Lett. **85**, 2506 (2000).
[11] D. Horváth, T. Bánsági Jr., and Á. Tóth, J. Chem. Phys. **117**, 4399 (2002).
[12] A. De Wit, Phys. Fluids **16**, 163 (2004).
[13] J. Yang, A. D'Onofrio, S. Kalliadasis, and A. De Wit, J. Chem. Phys. **117**, 9395 (2002).
[14] S. Kalliadasis, J. Yang, and A. De Wit, Phys. Fluids **16**, 1395 (2004).
[15] I. Nagypál and I. R. Epstein, J. Phys. Chem. **90**, 6285 (1986).
[16] R. K. Miller and A. N. Michel, *Ordinary Differential Equations* (Academic Press, New York, 1982).
[17] A. Tóth, D. Horváth, and W. van Saarloos, J. Chem. Phys. **111**, 10964 (1999).
[18] D. Horváth, A. Tóth, and K. Yoshikawa, J. Chem. Phys. **111**, 10 (1999).
[19] Z. Viranyi, A. Szommer, A. Tóth, and D. Horváth, Phys. Chem. Chem. Phys. **6**, 3396 (2004).